VHF Doppler Radar Observations of Buoyancy Waves Associated with Thunderstorms

DAREN LU,[1] T. E. VANZANDT AND W. L. CLARK

Aeronomy Laboratory, National Oceanic and Atmospheric Administration, Boulder, CO 80303

(Manuscript received 17 December 1982, in final form 11 August 1983)

ABSTRACT

The Platteville VHF Doppler radar, located on the Colorado piedmont near Platteville, Colorado, continuously measured the vertical wind velocity during a 12-day period in late July and early August 1981. Measurements were made every 2.5 min on the average with range gates centered at 3.3, 5.7, 8.1, 10.5, 12.9, 15.3, 17.7, and 20.1 km above sea level.

Periods of active thunderstorms were identified from the PPI maps from the National Weather Service 10 cm weather radar at Limon, Colorado. When no thunderstorm activity was present, the vertical velocity fluctuations were small and erratic. But a few hours after strong thunderstorm activity began, large quasi-sinusoidal wave trains with periods of about 40 min were observed. Power spectra of the vertical velocity time series showed enhancements at all frequencies during thunderstorm activity, but for periods longer than 30 min the enhancements were larger, particularly for the mid-tropospheric range gates from 5.7 to 12.9 km.

Some of the implications of these observations on the relations between thunderstorms and buoyancy waves in the free atmosphere are discussed.

1. Introduction

It has been recognized that the relation between buoyancy waves (internal gravity waves) and thunderstorms may be important in at least two respects: first, because buoyancy waves may affect the dynamics of thunderstorms and, second, because thunderstorms may contribute to the energy of the atmospheric buoyancy wave field.

Many different techniques have been used for studying atmospheric buoyancy waves in general and their relation to thunderstorms in particular: barograph and microbarograph arrays (Curry and Murty, 1974; Uccellini, 1975; Balachandran, 1980; Stobie *et al.*, 1983), acoustic sounders (Brown and Hall, 1978), satellite imagery (Erickson and Whitney, 1973; Stobie, 1975; Thomas *et al.*, 1975; Ley and Peltier, 1981), FM-CW radars (Gossard *et al.*, 1970), pulsed Doppler radars (VanZandt *et al.*, 1979; Röttger, 1980; Larsen *et al.*, 1982); see also Einaudi *et al.* (1979). In spite of the variety of techniques, our knowledge of the relation between buoyancy waves and thunderstorms is still rudimentary, partly because of the limitations of the various techniques and partly because of the inherent difficulty of observation of a phenomenon such as a thunderstorm that is sporadic in both space and time. Different observers have found buoyancy waves associated with thunderstorms with periods ranging between 5 min and 3 h and with phase speeds ranging from 12 to 30 m s^{-1}. The limits of these ranges may be partly due to the limitations of the measurement techniques, so that periods and phase speeds outside these ranges are certainly possible.

This paper reports further observations of buoyancy waves associated with thunderstorms. These observations were made with a VHF pulsed Doppler radar. This technique has the advantage that it measures a profile of wave motions versus altitude with a rapid cadence over long periods of time (Green *et al.*, 1979). This permits observation of the spatial and temporal morphology of waves throughout the troposphere, which has not been done with any other technique. The results in the present paper must be considered preliminary, however, since the experimental arrangement was not adequate to obtain the phase velocity of the waves.

The mechanism or mechanisms that relate buoyancy waves and thunderstorms is still uncertain. It has been suggested that buoyancy waves are generated by thunderstorms. Three mechanisms have been discussed: penetrative convection (Pierce and Coroniti, 1966; Stull, 1976), release of latent heat (Ley and Peltier, 1981), and shear instability of the outflow from a thunderstorm (Stobie, 1975; Balachandran, 1980). Stobie *et al.* (1983), on the other hand, suggest that in their case a wave generated by jet-stream shears initiated convection along its path, which then reinforced the wave. The implications of the present observations on these mechanisms are considered in Section 5.

[1] Permanent affiliation: Institute of Atmospheric Physics, Academia Sinica, Beijing, People's Republic of China.

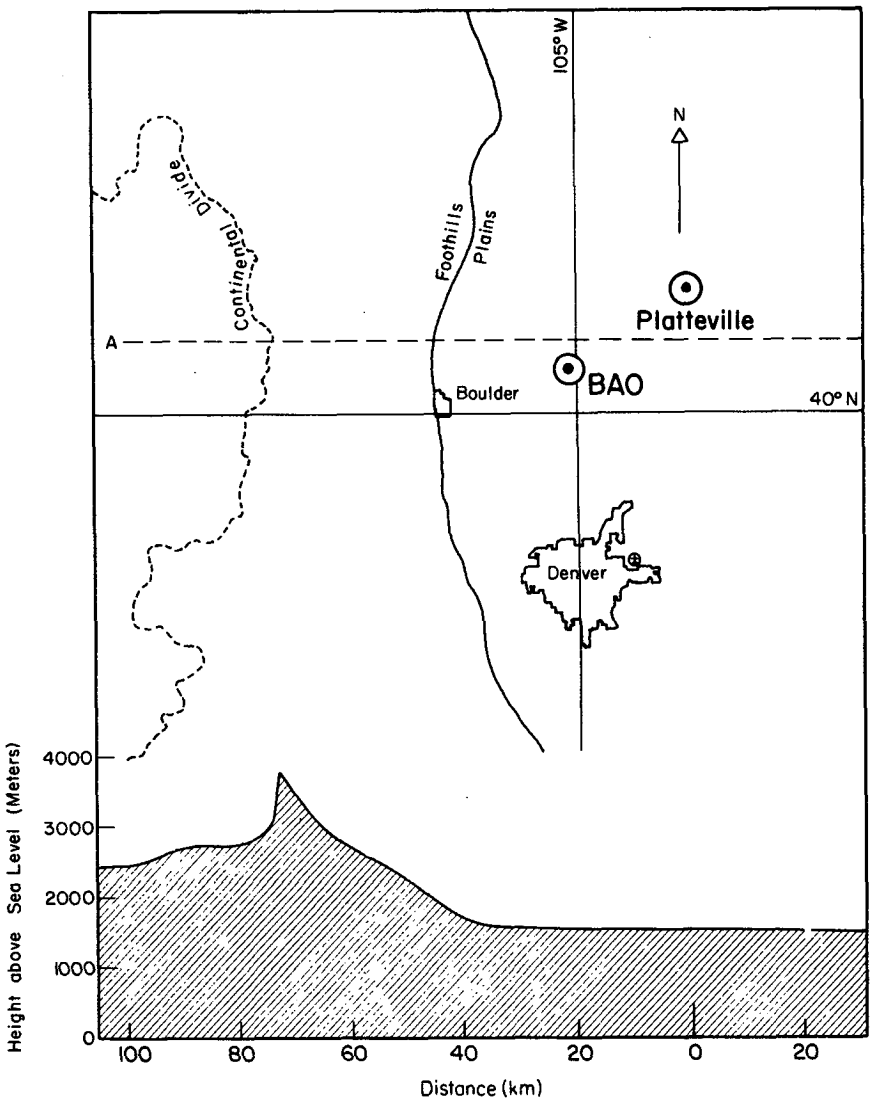

FIG. 1. Map showing the locations of the Platteville VHF Doppler radar and the Boulder Atmospheric Observatory (BAO), site of the microbarograph array. A cross section of the terrain is shown at the bottom.

2. Observations

Field observations were made from late July to early August 1981, during the period of maximum thunderstorm frequency in northeastern Colorado, as determined from the statistics of rainfall. The principal instrument used was the Platteville VHF Doppler radar[2] located on the Colorado piedmont near Platteville, Colorado, (see Fig. 1) with local relief of less than 100 m. The radar made observations both in the zenith and at a slant, from which both the vertical and horizontal wind components can be inferred. But in this paper only the vertical observations are used, because buoyancy waves are much more evident in this component and because the radar has greater altitude range in the vertical.

The radar range gates are roughly Gaussian in shape, so that they can be characterized by their center altitudes and their half-power widths. The Platteville radar range gates were centered 2.4 km apart at altitudes of 3.3, 5.7, 8.1, 10.5, 12.9, 15.3, 17.7, 20.1 and 22.5 km. No useful data were obtained by the 22.5 km range gate. The center to half-power width of the range gates was 1.2 km. Thus, adjacent range gates have considerable overlap, so that a strong echoing

[2] The Platteville radar is a joint facility of the Aeronomy and the Wave Propagation Laboratories of NOAA.

TABLE 1. Platteville radar system parameters.

Latitude	40°11′N
Longitude	104°44′N
Elevation	1536 m
Frequency	49.920 MHz
Peak pulse power	~15 kW
Average power	133 W
Pulse width	16 μs
Range resolution	2.4 km
Antenna area	100 × 100 m²
Beamwidth (two-way)	~2°

layer located in the region of overlap will be seen in both range gates.

The radar system parameters are given in Table 1. Further details are given by Ecklund *et al.* (1979). The basic data product for this type of radar is a Doppler spectrum that represents the average velocity spectrum over a certain length of time. In the present study alternate spectra were averaged over 157 s and 78 s and the cycle was repeated every 307 s. From each spectrum the mean vertical velocity was scaled. The resulting time series were then edited to remove spurious values due to aircraft, meteors, etc. Any echo whose velocity or strength was inconsistent with neighboring values was assumed to be spurious.

This radar system gathered data almost continuously for 12 days. The radar data were supplemented by surface pressure observations made by the microbarograph array operated by the Wave Propagation Laboratory at the Boulder Atmospheric Observatory (BAO) (see Fig. 1).

In order to identify thunderstorms and periods of thunderstorm activity, we used the PPI maps from the conventional 10 cm weather radar operated by the National Weather Service (NWS) at Limon, Colorado, (about 135 km southeast of the radar) and visible and infrared images taken by the GOES West (39°12′N, 103°42′W) satellite and recorded by the Atmospheric Sciences Department of the Colorado State University in Fort Collins, Colorado. Routine NWS radiosonde ascents from Denver (about 50 km from the radar) were used to determine the height of the tropopause.

Times will be given in Mountain Standard Time (MST) (=105°W time) (which is GMT less seven hours).

3. Analysis

The time series of vertical velocities measured by the Platteville radar for the entire 12 day period are shown for each range gate in Fig. 2. Each point is a 15 min average of the Doppler spectra. The vertical velocities fluctuate about a mean value that is approximately zero. The background level of fluctuation in the troposphere up to 12.9 km was of the order of 0.5 m s^{-1} peak-to-peak. But occasionally the level of fluctuation increased greatly for periods that lasted from several to more than 10 h. It will be seen later (Figs. 5 and 9) that these enhanced fluctuations are typically quasi-sinusoidal.

In order to study the relation between the periods of large fluctuations and periods of local thunderstorm activity, we used the Limon radar PPI maps to divide the 12 day period into "thunderstorm-active" and "thunderstorm-quiet" periods. This division is obviously rather subjective, but it was done without reference to the Platteville radar data. The thunderstorm-active periods are indicated on Fig. 2 just above the abscissal axis.

It can be seen that the periods of enhanced fluctuations usually correspond to thunderstorm-active periods, but with a lag of one to several hours. It seems very likely, therefore, that the coherent wave trains are associated with thunderstorms. In order to test this hypothesis further, we shall consider two particular cases and then discuss the statistics of several cases.

a. Case I, 1–2 August 1981

The synoptic situation on 1–2 August was as follows. On the 1700 MST 1 August (0000 GMT 2 August) surface chart (Fig. 3a) there was a stationary front extending from southern Idaho to Minnesota. The 300 mb chart (Fig. 3b) showed that Colorado was located south of a weak jet stream. This situation persisted over at least two days centered on 0000 GMT 2 August.

On the Limon radar PPI maps widely scattered echoes first appeared at about 1300 MST, and then after about 1500 MST stronger and more extensive echoes appeared, resulting in an echo band aligned from southwest to northeast, with the nearest point being about 50 km southeast of Platteville. Satellite

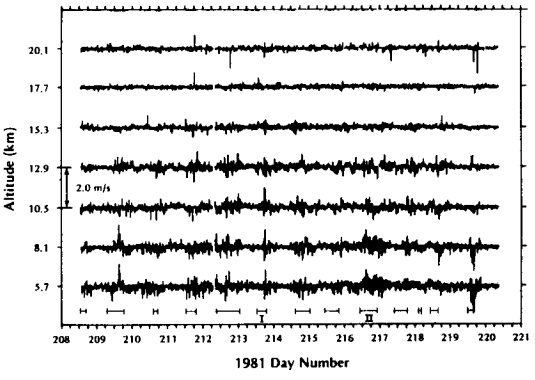

FIG. 2. Time series of vertical velocity during the 12 day period of observations. Each point is the average velocity for 15 min. Thunderstorm-active periods are indicated just above the abscissa. The altitude is above sea level. The day number is centered on 0000 MST of the day. Day 209 is 28 July, day 220 is 8 August.

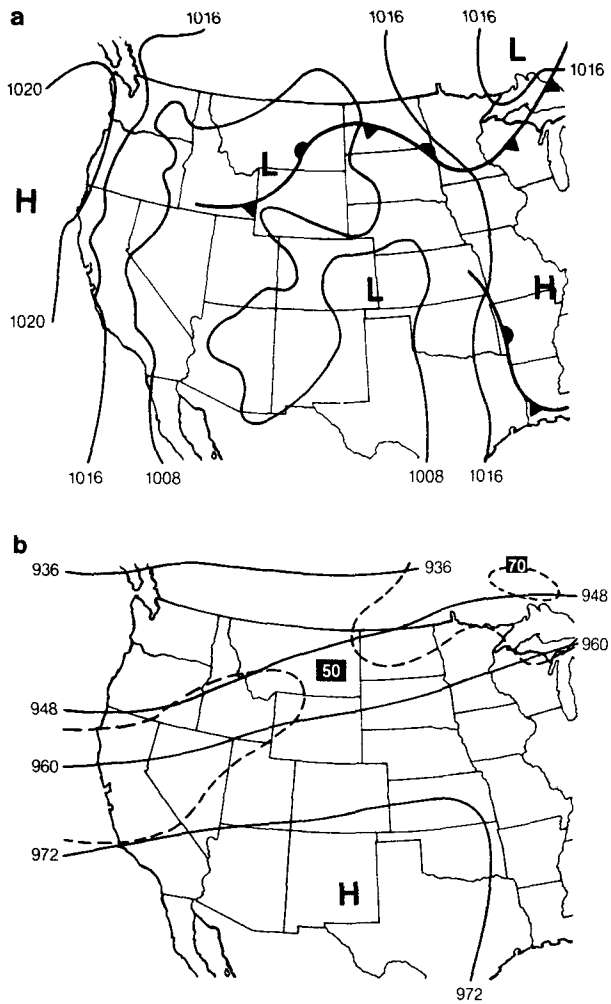

FIG. 3. (a) The surface synoptic chart for 1700 MST 1 August (0000 GMT 2 August) 1981. (b) The 300 mb synoptic chart for the same time.

images were available from 1133 to 1704 MST. From the infrared images it was found that at about 1500 MST the strongest local thundercloud was located at the northeastern end of the echo band, about 100–130 km northeast of Platteville, and at 1700 MST, about 150–180 km northeast. According to the Limon radar this thunderstorm decayed at about 1800. This is taken to be the end of the thunderstorm-active period.

The thunderstorm activity over a wider area than is visible from the Limon radar is shown in the maps in Fig. 4 taken from the NWS Radar Summary maps. Particularly notable are the appearance of an intense thunderstorm in the Oklahoma panhandle at 1135 MST and the development of storms in Nebraska from 1235 MST onward.

The time series of vertical velocities observed by the Platteville radar on 1–2 August are shown in Fig. 5. In this graph there are two points every 307 s. It is apparent that the quasi-sinusoidal wave train started between 1700 and 1800, two or three hours after the beginning of extensive local thunderstorm activity, and continued until about 2300, about five hours after the end of local thunderstorm activity at 1800. These oscillations can be seen in three or four range gates, with little if any phase change. Their amplitude was roughly constant at 5.6, 8.1, and 10.5 km, smaller at 12.9 km, weak at 15.3 km, and absent at 17.7 km. On this day the tropopause altitude ranged from 15.2 to 15.6 km, as determined from the routine Denver radiosonde ascents at 1700 MST 1 August and 0500 MST 2 August (0000 GMT and 1200 GMT 2 August). Since the lower half-power altitude of the 15.3 km range gate is at about 14.1 km, it is quite possible that the quasi-sinusoidal oscillations were entirely absent from the stratosphere.

In order to analyze these variations in more detail, power spectra were calculated from the time series for the wave-active period from 1700 to 2300 MST and for the following quiet period from 2300 to 2900 MST 1 August. (Times greater than 2400 are used to simplify the designation of time intervals.) Only the more precise velocities derived from the 157 s Doppler spectra were used in the analysis. The power spectra were calculated by first examining the time series and flagging all points in error (e.g., points contaminated by echoes from airplanes, meteors, etc.). The mean was then calculated and removed. Next, the autocorrelation function was calculated, ignoring all lags containing a flagged data value. This was transformed to the power spectrum, and a three-point smoothing applied (weights = 0.25, 0.5, 0.25) to obtain the final power spectrum shown in Fig. 6. It should be noted that the removal of the mean has decreased the power in the extreme low end of the frequency band.

During the quiet period the spectra are nearly white, although there are persistent peaks at about 20 and 50 min. During the active period the variance is increased at most altitudes. At 5.7, 8.1, and 10.5 km the power is greatly enhanced (by an order of magnitude) for periods longer than about 20 min; at shorter periods there is little or no change. At 12.9 and 15.3 km, on the other hand, the power is enhanced at all periods, but only by a factor of about 3. At 17.7 km there is no significant change. At 3.3 km the variance is actually reduced, but with a tendency for the power to be confined to three peaks, centered at about 12, 20, and 60 min.

Wave analysis of the BAO microbarograph data from 2000 to 2240 MST also showed a spectral peak at 1024 s (17.1 min), in good agreement with the radar data from 3.3 km. Analysis showed that this wave came from an azimuth of 120° (clockwise from north) with a phase velocity of about 10 m s^{-1}. The wavelength was then about 10 km. But since the microbarograph

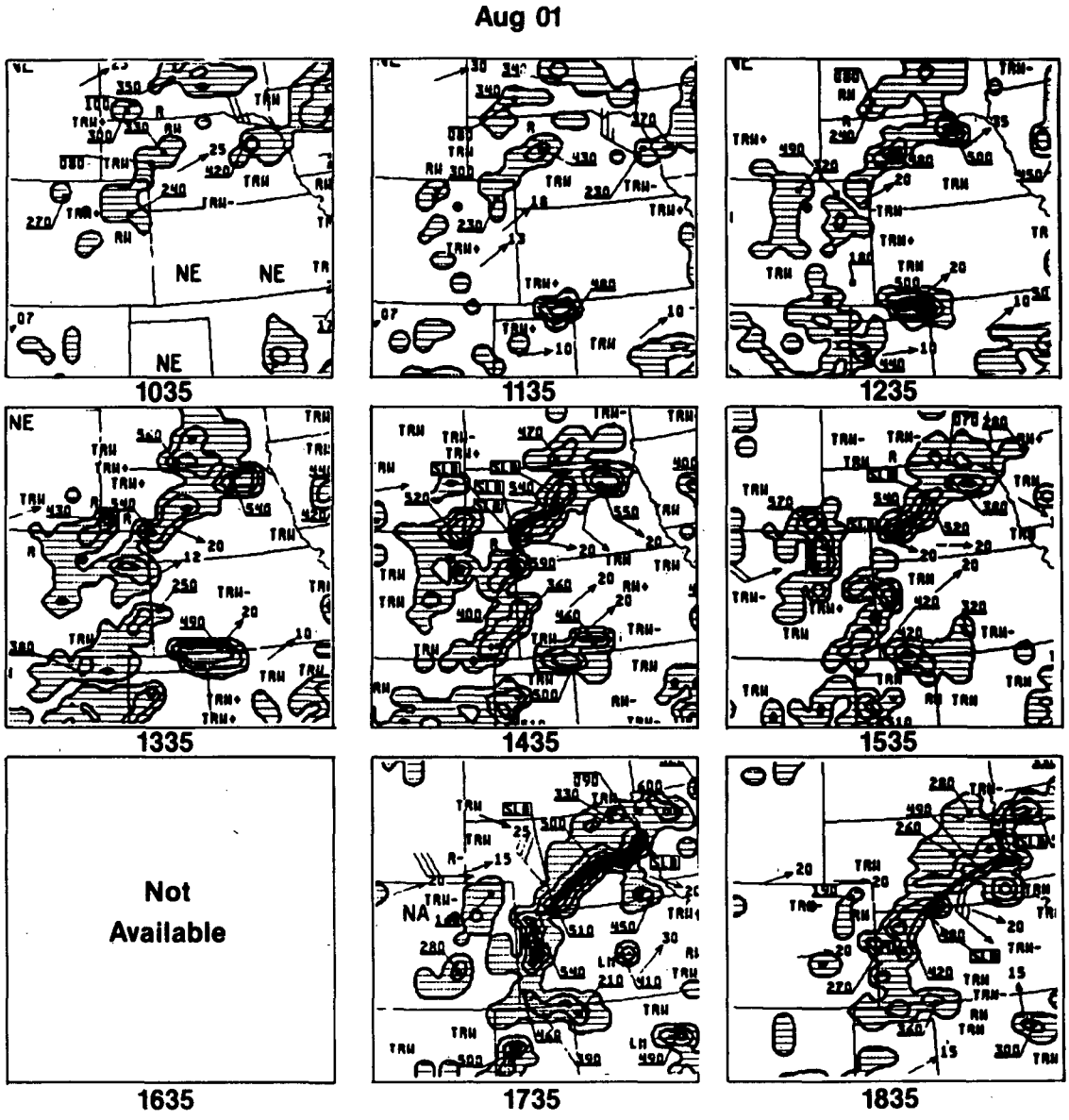

FIG. 4. Radar summary charts from 1035 to 1835 MST 1 August (1735 GMT 1 August to 0135 GMT 2 August) 1981. The solid dot in northeastern Colorado indicates the location of the Platteville radar. Each map is about 1150 km on a side.

array at BAO is a triangle with sides of only about 300 m, much less than the calculated wavelength, this value is very approximate.

b. Case II, 4–5 August 1981

The synoptic situation on 4–5 August was similar to that on 1–2 August. From 1700 MST 3 August (0000 GMT 4 August) to 1700 MST 4 August (0000 GMT 5 August) a stationary front extended from central Wyoming to the Great Lakes (see Fig. 7a). Then by 1700 MST 5 August (0000 GMT 6 August) the front had moved southward to extend from central Colorado to central Illinois. The 300 mb chart (Fig. 7b) again showed that Colorado was located south of a weak jet stream.

Convective echoes began to appear on the Limon PPI maps at about 1000 MST, 4 August. After about 1100 MST stronger echoes appeared north and east of Platteville and continued until 2225 MST when the last strong echo band moved to the east off of the Limon PPI map.

In the radar summary maps shown in Fig. 8, strong convective activity appeared at 0835 in southwestern

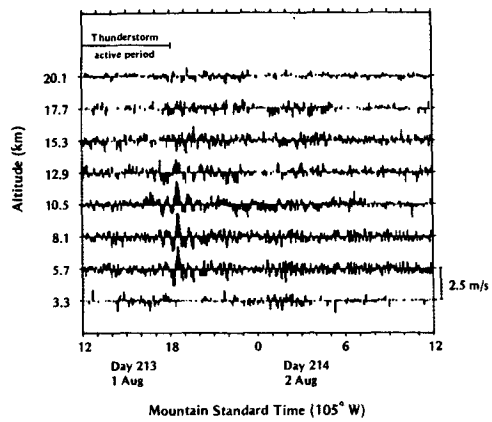

FIG. 5. Time series of vertical velocity corresponding to thunderstorm-active period Case I. Each point is the average velocity for 307 s. The duration of thunderstorm-active period I is shown along the top of the figure.

South Dakota, prior to the activity in northeastern Colorado.

The vertical velocity time series from the Platteville radar observations of 4–5 August are shown in Fig. 9. It is clear that strong, quasi-sinusoidal vertical oscillations started at about 1400 MST, about 3 h after the beginning of the thunderstorm-active period, and continued to at least 2900 MST. These oscillations are most evident in the 5.7 and 8.1 km range gates, but they are also detectable in the 3.3, 10.5, 12.9, and even perhaps in the 15.3 range gates. As in Case I the oscillations were vertically coherent, with little or no phase change with altitude.

The power spectra during the wave-active period, 1400 to 2900 MST 4 August and for the preceding quiet period, 0000 to 1200 MST 4 August, are shown in Fig. 10. During the active period the tropospheric spectral power in the range gates from 3.3 to 10.5 km is enhanced at periods from about 25 min to 1.5 h. (Also, in the 3.3 km range gate there is an enhancement in periods between about 10 and 14 min.) The most prominent spectral peaks are at 40 and 60 min, which correspond to the most evident oscillations in the time series. There is no significant enhancement in the 15.3 and 17.7 km range gates.

Wave analysis of the BAO microbarograph data was done for three periods, 1500–1840 MST, 2000–2140 MST, and 2330–2500 MST, all on 4 August. During the first two periods the power spectra had peaks at 20 min and shorter periods, and the waves were found to come from the northeast and east (the direction of active thunderstorms) with phase velocities of 3–5 m s^{-1} for the first period and 4–6 m s^{-1} for the second. In the third period there were quasi-monochromatic waves coming from the northwest with periods of 6–8 min and phase velocities of 10–16 m s^{-1}. These latter waves were identified as being typical stable boundary layer buoyancy waves. They appear to be uncorrelated with the tropospheric waves.

4. Statistical studies

Cases I and II exhibit most of the features of thunderstorm-generated buoyancy waves that we have seen

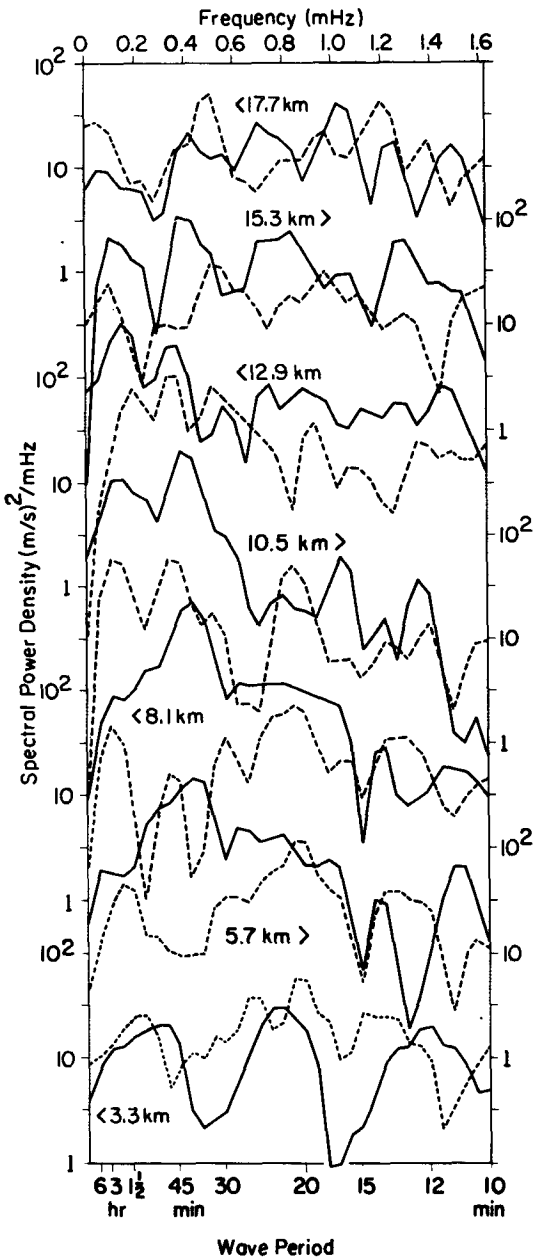

FIG. 6. Power spectra of the active period from 1700 to 2300 MST 1 August in Fig. 5 (solid lines) and for the following quiet period from 2300 to 2900 MST 1 August (dashed lines). The scale for each altitude is indicated by the caret, ⟨ or ⟩.

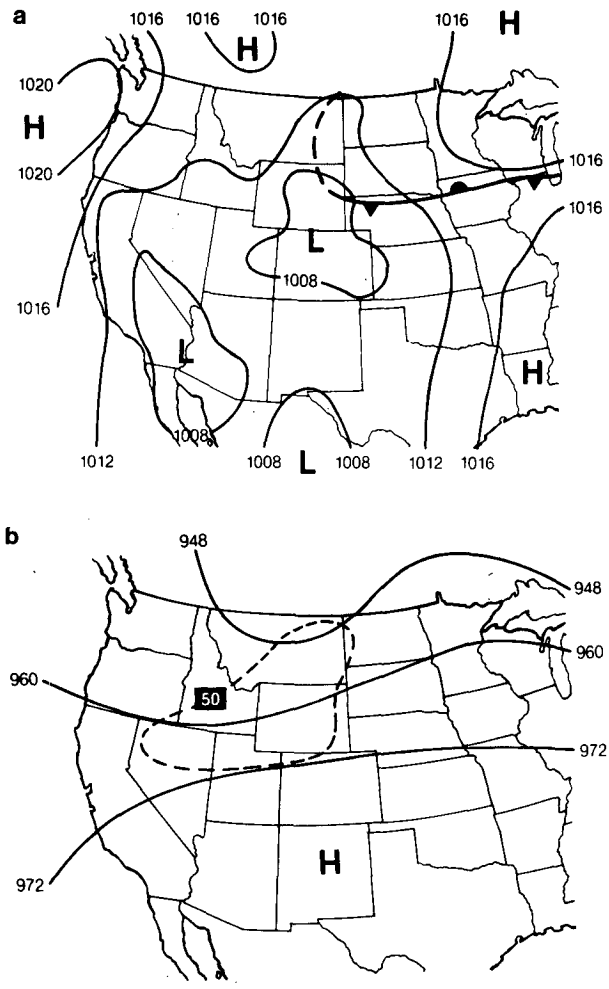

FIG. 7. (a) The surface synoptic chart for 1700 MST 4 August (0000 GMT 5 August) 1981. (b) The 300 mb synoptic chart for the same time.

in our observations. Therefore, rather than discussing in detail the entire 12 days of continuous observations, we will consider only their statistical features.

a. Enhancement as a function of frequency

In the discussion of Cases I and II it was noted that the power spectra were enhanced in the troposphere during wave-active periods, particularly at periods longer than about 20 or 30 min. The average enhancement as a function of period is shown in Fig. 11 for three active periods versus three nearby quiet periods, which are listed in Table 2. The variance in each frequency interval is the integral of the power spectrum over that interval. The variance is significantly enhanced at all frequencies at all heights, except for the 15 to 30 min range at 3.3 km and the stratospheric 17.7 km range gate. For periods longer than 30 min the enhancements are large, particularly for the midtropospheric range gates from 5.7 to 10.5 km. For periods shorter than 30 min the enhancements are smaller.

b. Enhancement as a function of altitude

The enhancement as a function of altitude is shown in Fig. 12 as the ratio of active to quiet variance for six active and four quiet periods. Here the variance is the integral over the entire spectrum. The time periods used, listed in Table 2, include not only the paired active and quiet periods of Fig. 11, but also some unpaired periods. The enhancement would be even more striking if one of the wave-active periods were omitted, since during that period the local thunderstorm activity was weak and the variance was small. The enhancement is largest in midtroposphere, from the 5.7 to the 12.9 km range gates.

Over the entire 12 day period the average height of the tropopause (determined from routine Denver NWS radiosonde ascents) was 15.3 km and it ranged from 14.2 to 16.2 km, as indicated in Fig. 12. There was no enhancement in the purely stratospheric 17.7 km range gate, and the rather small enhancement in the 15.3 km range gate may have been entirely due to tropospheric waves.

c. Vertical coherence

The strong wave trains observable in the wave-active periods usually exhibit coherence versus altitude. Occasionally the waves were coherent between four consecutive altitudes (as in Case I from 1700 to 2100 MST 1 August. In many cases the waves were coherent only between adjacent range gates, which could be the result of the overlap of the range-gate filter functions (see Section 2).

Phase variation versus altitude could be detected only rarely, which suggests that the dominant wave trains were ducted.

5. Discussion

Based on the analyses of the preceding sections, the main characteristics of the buoyancy waves associated with thunderstorms can be summarized briefly as follows:

1) During thunderstorms the power spectrum in the surrounding troposphere is enhanced principally at periods longer than about 30 min, with the largest enhancements being in the range from 30 min to 1 h in the midtroposphere. The largest enhancements are principally due to large quasi-sinusoidal waves. There is no evidence of enhancement of the spectrum in the lower stratosphere.

2) The variance, obtained by integrating the power spectrum over frequency, is enhanced in the entire

FIG. 8. Radar summary charts from 0835 to 2235 MST 4 August (1535 GMT 4 August to 0535 GMT 5 August) 1981. The charts for 1735, 1935, and 2135 MST have been omitted. The solid dot in northeastern Colorado indicates the location of the Platteville radar. Each map is about 1150 km on a side.

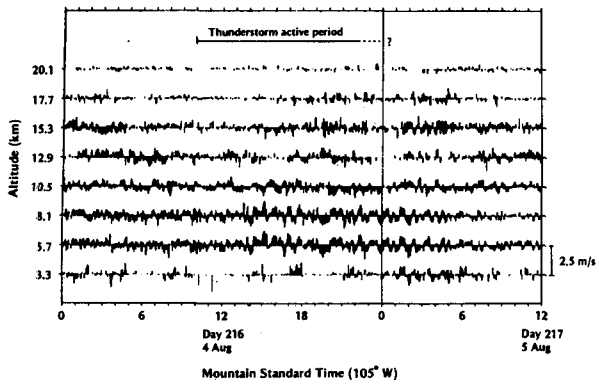

FIG. 9. Time series of vertical velocity corresponding to thunderstorm-active period Case II. Each point is the average velocity for 307 s. The duration of thunderstorm-active period II is shown along the top of the figure. The question mark at the end of the period indicates that the end of the active period is not known, since the active region moved off of the Limon PPI map at 2225 MST.

troposphere, but particularly in the midtroposphere, where the enhancement can be as large as a factor of 10 in some cases.

3) Little or no coherence is seen between waves observed at the ground and in the troposphere.

Although the present observations are inadequate to describe fully the relation between the observed buoyancy waves and thunderstorms, particularly because the phase velocity was not measured, it is nevertheless worth discussing some of the implications of our observations.

It was mentioned in the Introduction that the mechanism or mechanisms that relate buoyancy waves and thunderstorms are still uncertain. Several authors have suggested various mechanisms by which buoyancy waves can be generated by thunderstorms. Stobie *et al.* (1983), on the other hand, suggest a more complicated interaction in which an impinging wave initiates convection that in turn reinforces the wave (or generates new waves by one of the other mechanisms).

If it had been possible in this study to measure the phase velocity of the waves, such as those in Cases I and II, then the particular thunderstorms that acted as the sources of these waves could have been identified. The source storms would have to lie on or near the radius from the station in the direction from which the wave came, and they would have to lie on the range-time curve determined by the phase speed.

In the present study we have related the enhancements of the wave spectrum to local thunderstorm activity, that is, activity within the range of the Limon radar. The possibility cannot be excluded, however, that some of the wave activity could have been caused by earlier, more distant storms. For example, in Case I the wave train that started at about 1700 MST 1 August could have come from the storm that appeared in the Oklahoma panhandle on the 1135 MST radar summary map in Fig. 4 if the wave had traveled with a speed of 25 m s^{-1}, which is not unreasonable. Similarly, in Case II, the wave train that started at about 1400 MST could have come from the storm that appeared in southwestern South Dakota on the 0935

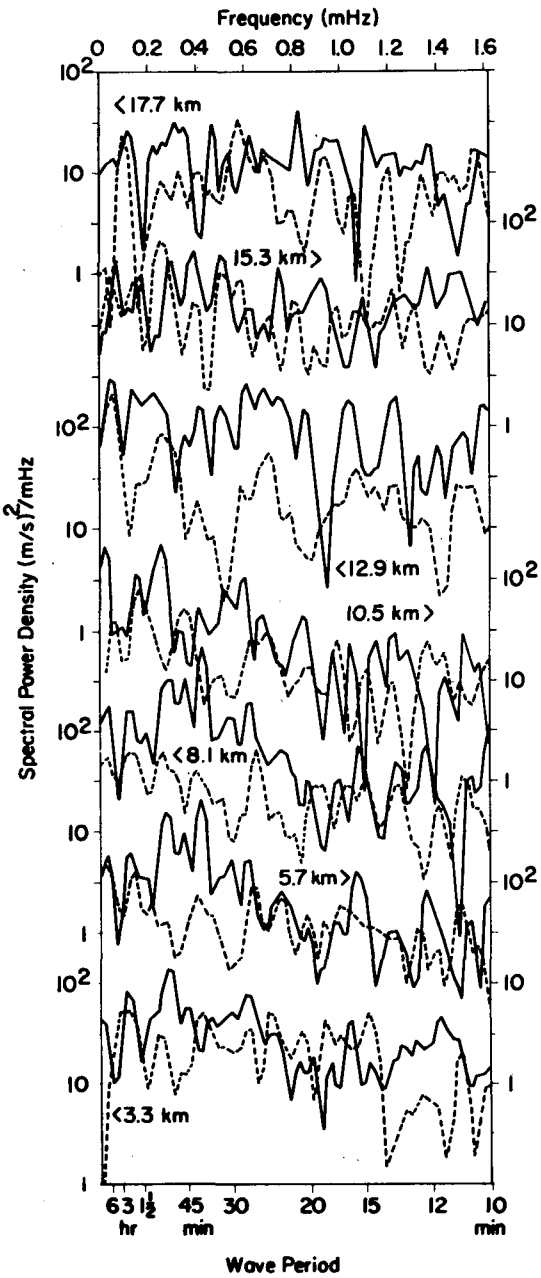

FIG. 10. Power spectra of the active period from 1400 to 2900 MST 4 August in Fig. 9 (solid lines) and for the preceding quiet period from 0000 to 1200 MST 4 August (dashed lines). The scale for each altitude is indicated by the left or right angle brackets.

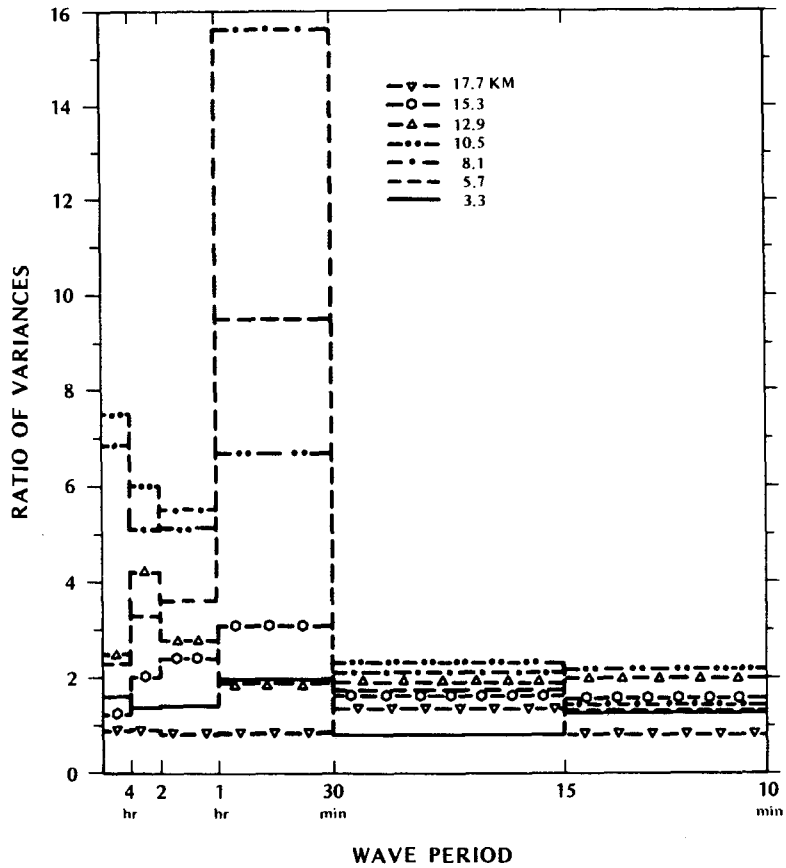

FIG. 11. The enhancement due to thunderstorm activity as a function of period. The ratio of the variance in each frequency interval during three wave-active periods (listed in Table 2) to the variance during three quiet periods (also listed in Table 2) is plotted.

MST Radar Summary map (Fig. 8) by travelling at a similar speed.

Identification of the source storms by means of measured phase velocities would permit testing the proposed source mechanisms by constructing dynamical models of the wave generation and propagation processes for particular cases. However, such a study will have to await observations by suitable arrays of radars.

Without knowledge of the phase velocity, it is possible to say only that the observed enhancements are more likely due to the mechanisms of penetrative convection or release of latent heat than to shear instability or wave reinforcement, simply because the former two mechanisms launch waves over a wide range of azimuths, while the latter two are much more directional.

Pierce and Coroniti (1966) and Curry and Murty (1974) suggested that the waves generated by penetrative convection would have frequencies near the local buoyancy (Brunt-Väisälä) frequency. Such oscillations are inconsistent with the present result that the principal enhancements are for periods longer than 30 min, which is considerably longer than the buoyancy period in the troposphere and lower stratosphere as calculated from the routine radiosonde data, except for occasional marginally stable or unstable layers with thicknesses

TABLE 2. Observational periods used in this study.

Active periods	Quiet periods
0900–2100 MST 31 July	0300–1500 MST 1 Aug, (11)
1700–2300 1 Aug, (11) (I)	2300–2900 1 Aug, (11) (I)
1500–2500 2 Aug, (11)	000–1200 4 Aug, (11) (I)
1200–2200 3 Aug	2100–3300 7 Aug
1400–2900 4 Aug, (11) (II)	
1300–2200 5 Aug	

(11) denotes that these periods were used in Fig. 11.
(I) and (II) denote that these periods were used in Case (I) or Case II.
Times greater than 2400 are used to simplify the notation.

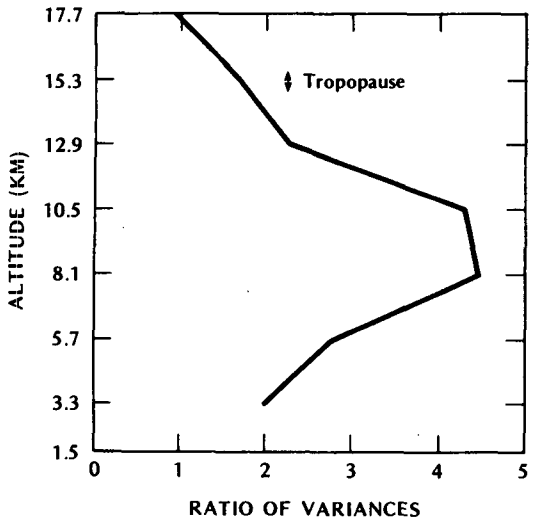

FIG. 12. The enhancement due to thunderstorm activity as a function of altitude. The ratio of the variance at each altitude during six wave-active periods (listed in Table 2) to the variance during four quiet periods (also listed in Table 2) is plotted. The range of radiosonde tropopause heights (14.2 to 16.2 km) during the entire 12 day period is indicated.

up to a few hundred meters, mostly in the lower troposphere. Also, oscillations near the buoyancy frequency have small phase and group velocities relative to the background flow (Gossard and Hooke, 1975).

Our observations also have implications on the interpretation of microbarograph records. The large difference between the spectra of thunderstorm-generated waves determined from radar observations and from microbarograph observations shows that it is impossible (or at least very difficult) to describe the principal characteristics of thunderstorm-generated waves from microbarograph observations alone. The differences between the ground and free-air spectra may be due either to ducting of the ground-observed waves in the boundary layer or to filtering by the boundary layer of downward propagating tropospheric waves. In the former case, the ground-observed spectra provide information on only part of the wave field. In the latter case, deconvolution of the effect of filtering in order to infer the tropospheric wave field is very difficult.

Thus, wave observations in the free air, for which pulsed Doppler radar is at present the most versatile measurement technique, are essential for a complete understanding of thunderstorm-generated waves.

Acknowledgments. The Platteville radar is a joint facility of the Wave Propagation Laboratory and the Aeronomy Laboratory of NOAA. We wish to thank W. L. Ecklund and B. B. Balsley for assistance in planning the experiment, R. G. Strauch for conducting the experiment, A. C. Riddle for off-line data processing, and K. J. Ruth for performing the spectral analyses. The microbarograph array data were provided by the Boulder Atmospheric Observatory group of the Wave Propagation Laboratory and the satellite data were provided under contract by the Department of Atmospheric Sciences of the Colorado State University. We are happy to acknowledge useful discussions with F. Einaudi, K. S. Gage and J. L. Green. One of the authors (D.R.L.) acknowledges NOAA and the Aeronomy Laboratory for providing the facilities for this research.

REFERENCES

Balachandran, N. K., 1980: Gravity waves from thunderstorms. *Mon. Wea. Rev.*, **108**, 804–816.

Brown, E. H., and F. F. Hall, Jr., 1978: Advances in atmospheric acoustics. *Rev. Geophys. Space Phys.*, **16**, 47–110.

Curry, M. J., and R. C. Murty, 1974: Thunderstorm-generated gravity waves. *J. Atmos. Sci.*, **31**, 1402–1408.

Ecklund, W. L., D. A. Carter and B. B. Balsley, 1979: Continuous measurement of upper atmospheric winds and turbulence using a VHF Doppler radar: Preliminary results. *J. Atmos. Terr. Phys.*, **41**, 983–994.

Einaudi, F., D. P. Lalas and G. E. Perona, 1979: The role of gravity waves in tropospheric processes. *Pure Appl. Geophys.*, **117**, 627–663.

Erickson, C. O., and L. E. Whitney, Jr., 1973: Picture of the month: Gravity waves following severe thunderstorms. *Mon. Wea. Rev.*, **101**, 708–711.

Gossard, E. E., and W. H. Hooke, 1975: *Waves in the Atmosphere.* Elsevier, 456 pp.

——, J. H. Richter and D. Atlas, 1970: Internal waves in the atmosphere from high-resolution radar measurements. *J. Geophys. Res.*, **75**, 3523–3536.

Green, J. L., K. S. Gage and T. E. VanZandt, 1979: Atmospheric measurements by VHF pulsed Doppler radar. *IEEE Trans. Geosci. Elec.*, **GE-17**, 262–280.

Larsen, M. F., W. E. Swartz and R. F. Woodman, 1982: Gravity-wave generation by thunderstorms observed with a vertically-pointing 430 MHz radar. *Geophys. Res. Lett.*, **9**, 571–574.

Ley, B. E., and W. R. Peltier, 1981: Propagating mesoscale cloud bands. *J. Atmos. Sci.*, **38**, 1206–1219.

Pierce, A. D., and S. C. Coroniti, 1966: A mechanism for the generation of acoustic-gravity waves during thunderstorm formation. *Nature*, **210**, 1209–1210.

Röttger, J., 1980: Structure and dynamics of the stratosphere and mesosphere revealed by VHF radar investigations. *Pure Appl. Geophys.*, **118**, 484–527.

Stobie, J. G., 1975: Gravity shear waves atop the cirrus layer of intense convective storms. Dept. Atmos. Sci., Colorado State University Rep., NASA CR-147140, 116 pp. [NTIS N76-22827].

——, F. Einaudi and L. W. Uccellini, 1983: A case study of gravity waves–convective storms interaction: 9 May 1979. *J. Atmos. Sci.*, **40**, 2804–2830.

Stull, R. B., 1976: Internal gravity waves generated by penetrative convection. *J. Atmos. Sci.*, **33**, 1279–1286.

Thomas, J. E., M. D. Days, J. D. Horn and R. L. Moore, 1975: Visual observation of propagating gravity waves on ATS III satellite film loops. Atmos. Sci. Laboratory, U.S. Army Electronics Command, Rep. ECOM-5553, 22 pp. [NTIS-AD/A-003843].

Uccellini, L. W., 1975: A case study of apparent gravity wave initiation of severe convective storms. *Mon. Wea. Rev.*, **103**, 497–513.

VanZandt, T. E., J. L. Green, W. L. Clark and J. R. Grant, 1979: Buoyancy waves in the troposphere: Doppler radar observations and a theoretical model. *Geophys. Res. Lett.*, **6**, 429–432.